Analyst

Electronic Supplementary Information

Triphenylamine indanedione as an AIE-based molecular sensor with one-step facile synthesis toward viscosity detection of liquids

Lingfeng Xu[1,2,*], Fangzhi Xiong[1], Minqing Kang[1], Yanrong Huang[3] and Kui Wu[4]

1 School of Chemistry and Chemical Engineering, Jinggangshan University, Ji'an, Jiangxi 343009, China

2 State Key Laboratory of Luminescent Materials & Devices, Guangdong Provincial Key Laboratory of Luminescence from Molecular Aggregates, College of Materials Science & Engineering, South China University of Technology, Guangzhou 510640, China

3 School of Food Science and Engineering, Guangdong Province Key Laboratory for Green Processing of Natural Products and Product Safety, South China University of Technology, Guangzhou 510640, China

4 School of Chemistry, Sun Yat-sen University, Guangzhou 510275, China

* Corresponding author. E-mail: rs7lfxu@outlook.com

Table of contents

Experimental section

1. Theoretical calculations

The calculations were performed using the Gaussian09 program, ground state structure of the sensor was optimized using time-dependent density functional theory (TD-DFT) by using the B3LYP/6-31G(d) level of theory.

2. Thickening effect analysis

Common food thickeners including the sodium carboxymethyl cellulose, pectin and xanthan gum with different mass concentrations (from 1 g/kg to 7 g/kg) were added into the distilled water with ultrasonic dispersion and corresponding thickening solutions were prepared. Before the test, bubbles in the solution were eliminated, and the stock solution of sensor DPTMID was diluted as 10 μM. The excitation wavelength was 500 nm, and emission spectra was recorded from 540 nm to 850 nm.

3. The Förster–Hoffmann equation

According to the previous studies,[1,2] the relationship between the fluorescence intensity of the molecular sensor DPBID & DPTMID and the viscosity can be determined by the following Förster–Hoffmann equation:

$$\log I = C + x \log \eta \tag{1}$$

where η represents the viscosity, I represents the fluorescence intensity of the molecular sensor DPBID at 588 nm & DPTMID at 670 nm, C is a constant, and x represents the sensitivity of the molecular sensor toward viscosity.
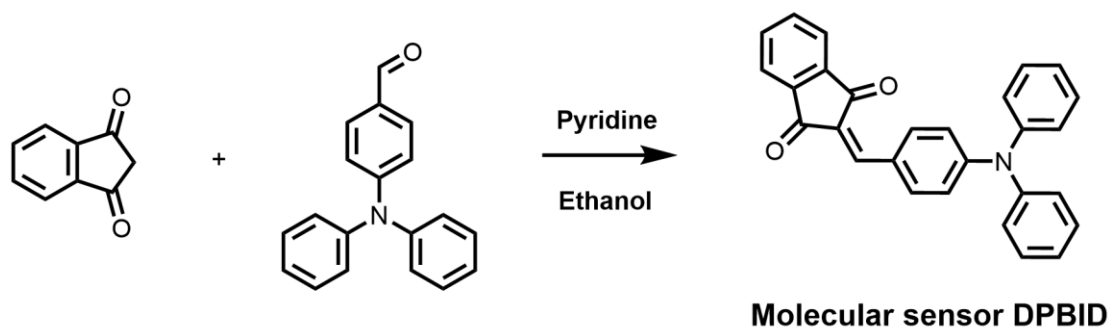
Scheme S1. Synthesis route of the molecular sensor DPBID.
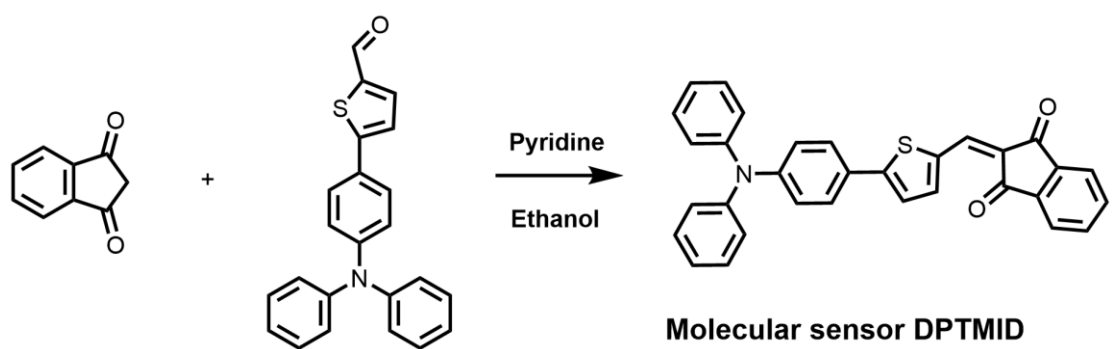
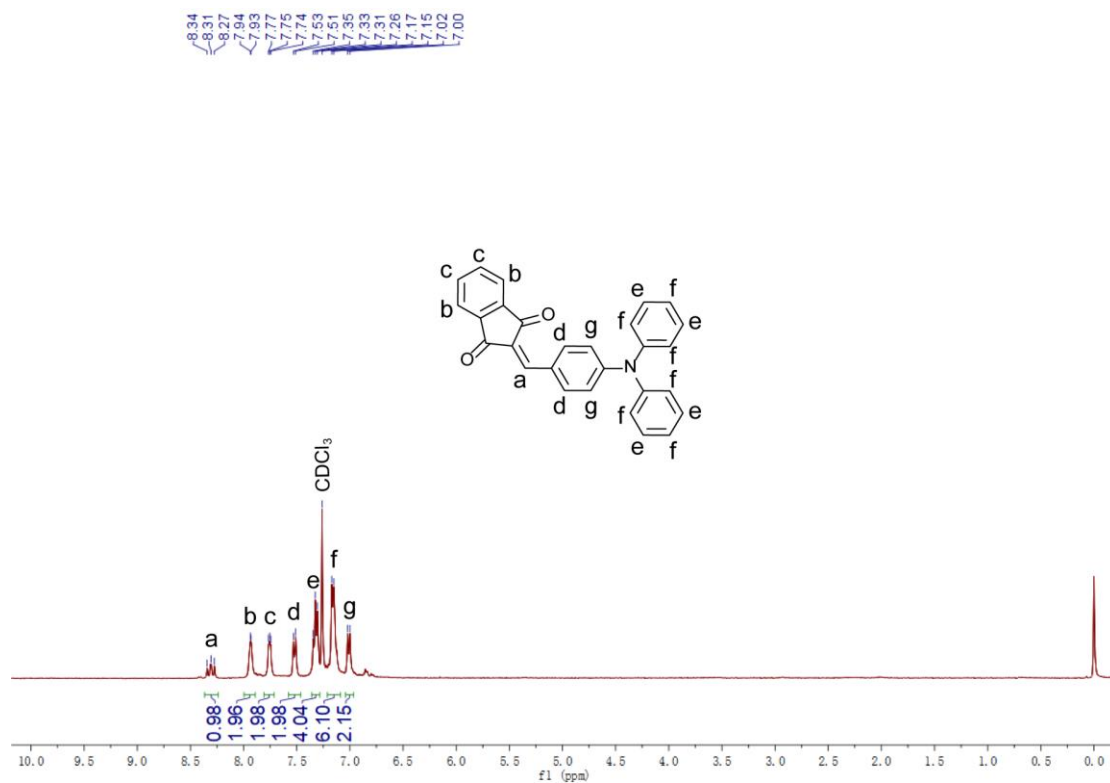**Scheme S2.** Synthesis route of the molecular sensor DPTMID.

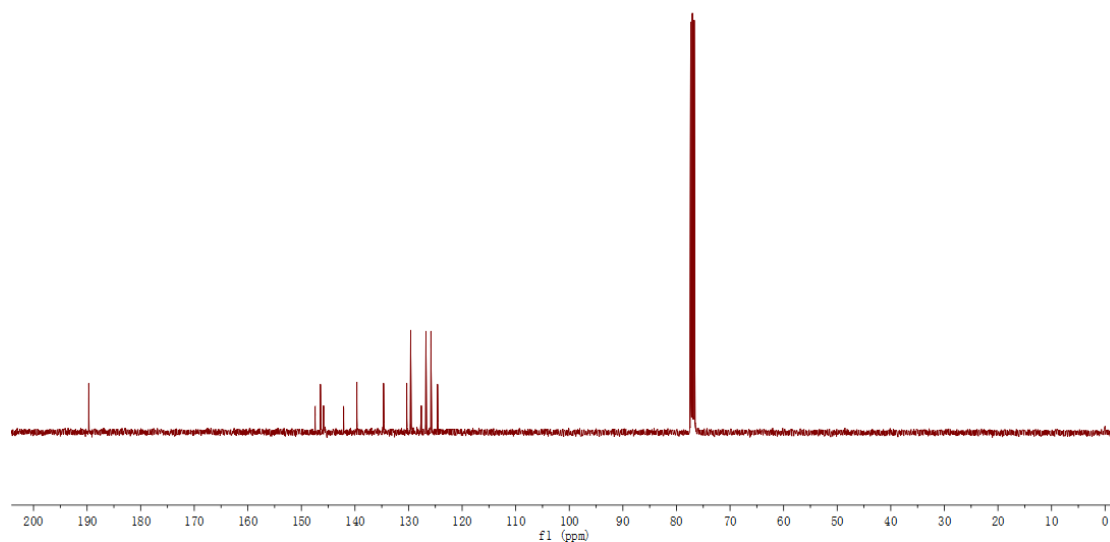**Fig. S1** ^{1}H-NMR spectrum of the molecular sensor DPBID in CDCl$_3$.

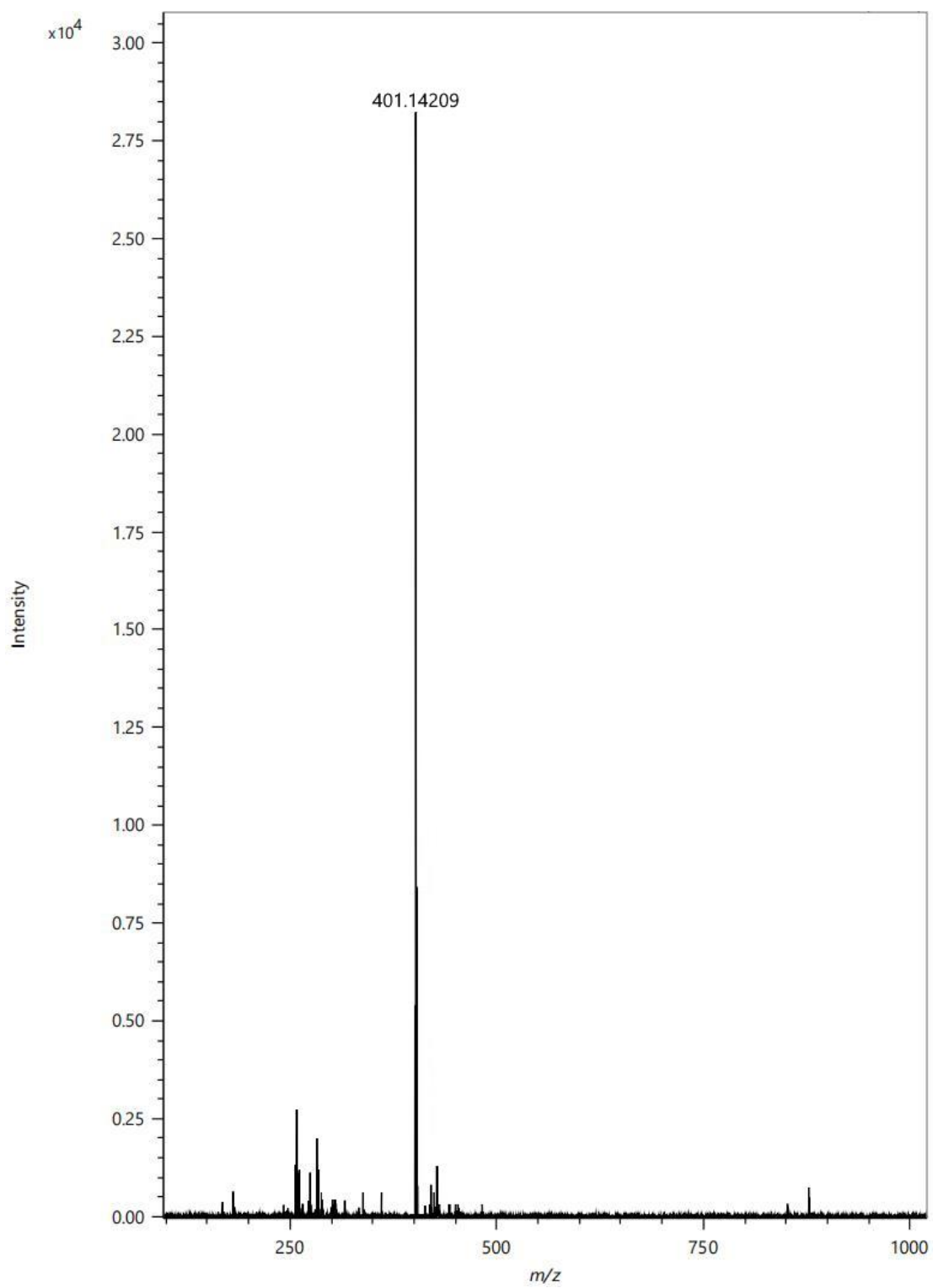**Fig.S2** ^{13}C-NMR spectrum of the molecular sensor DPBID in CDCl$_3$.

3

Fig. S3 HR mass spectrum of the molecular sensor DPBID. MS (ESI): m/z 401.14209
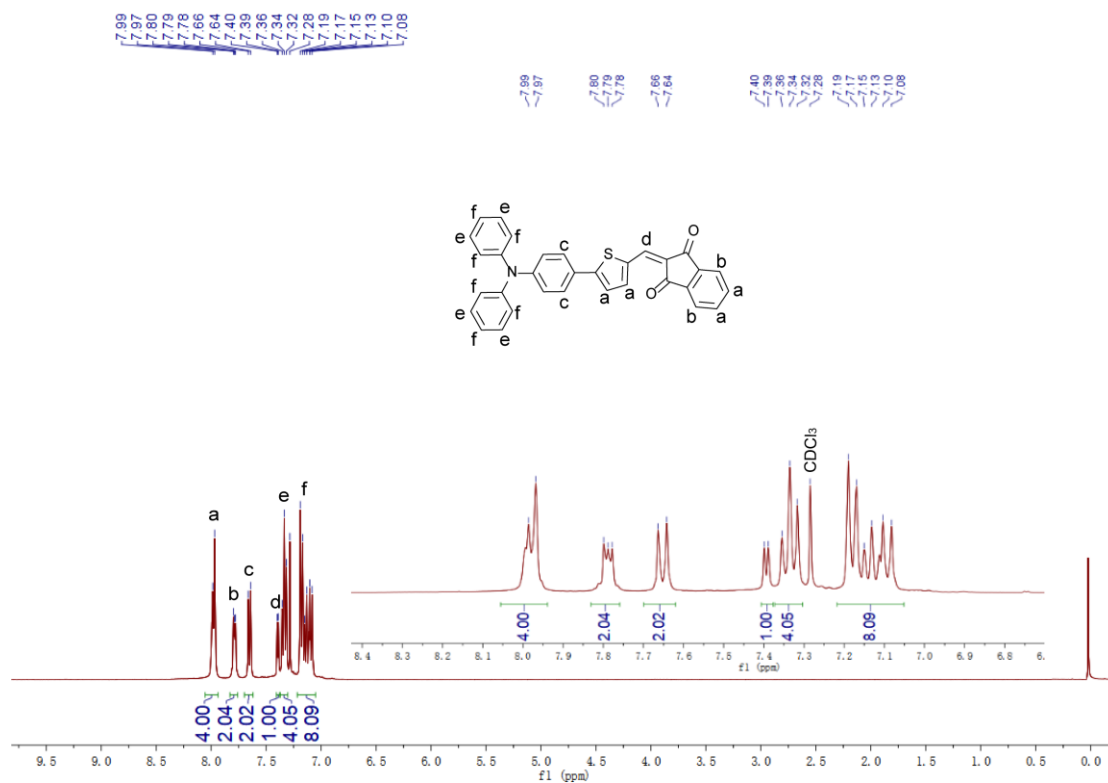
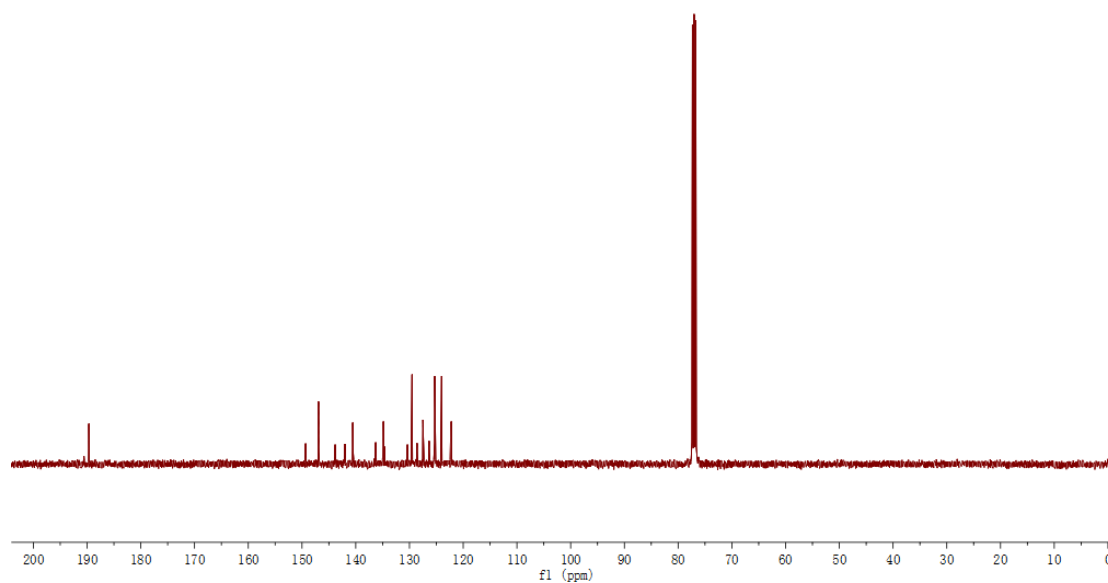**Fig. S4** ^{1}H-NMR spectrum of the molecular sensor DPTMID in CDCl$_3$.

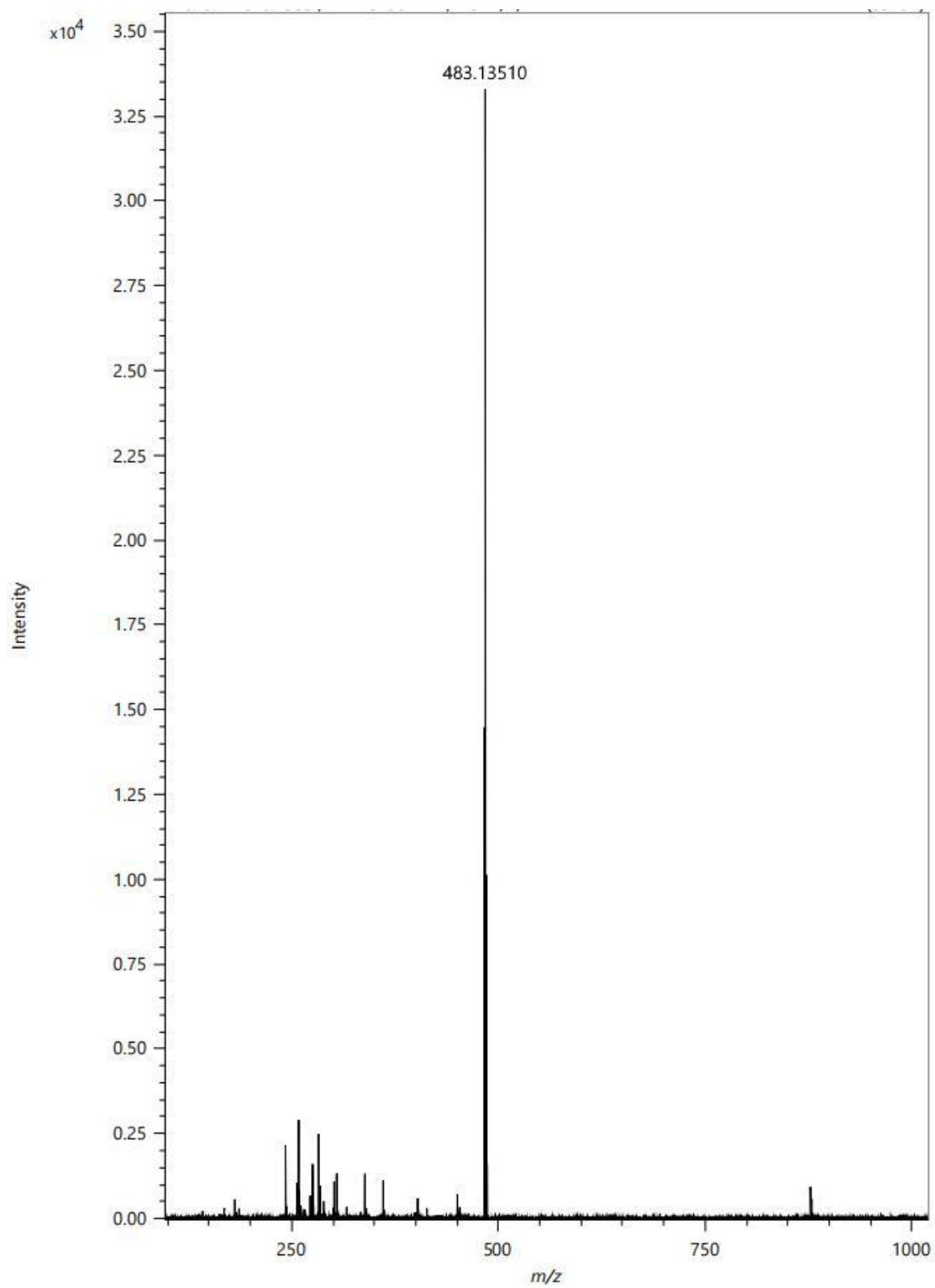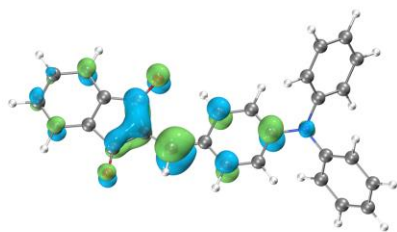**Fig. S5** ^{13}C-NMR spectrum of the molecular sensor DPTMID in CDCl$_3$.

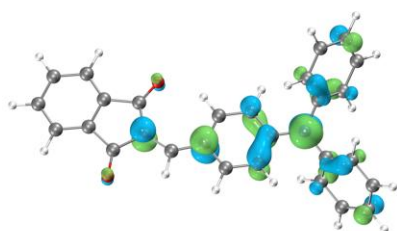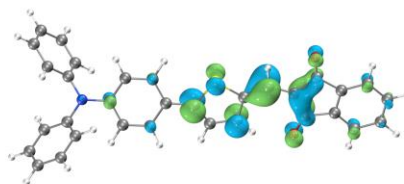**Fig. S6** HR mass spectrum of the molecular sensor DPTMID. MS (ESI): m/z

483.13510 [M]$^+$.
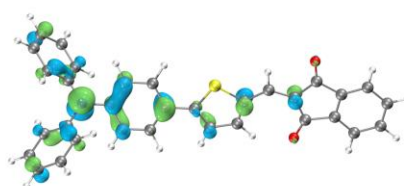
Fig. S7 (a) Stoke shift of the molecular sensor DPBID in low viscosity water (containing 1% DMSO). **(b)** Stokes shift of the molecular sensor DPTMID in high viscosity glycerol (containing 1% DMSO).

Fig. S8 (a) Fluorescent spectrum of the molecular sensor DPTMID (10 μM) in DMSO/water with different volume fractions of water (from 0% to 99%). (b) Plot of fluorescence intensity at 713.6 nm as a function of different volume fractions of water, λ_{ex}=500 nm. (c) Size distribution of rotor solution determined by using dynamic light scattering (DLS) method in water.
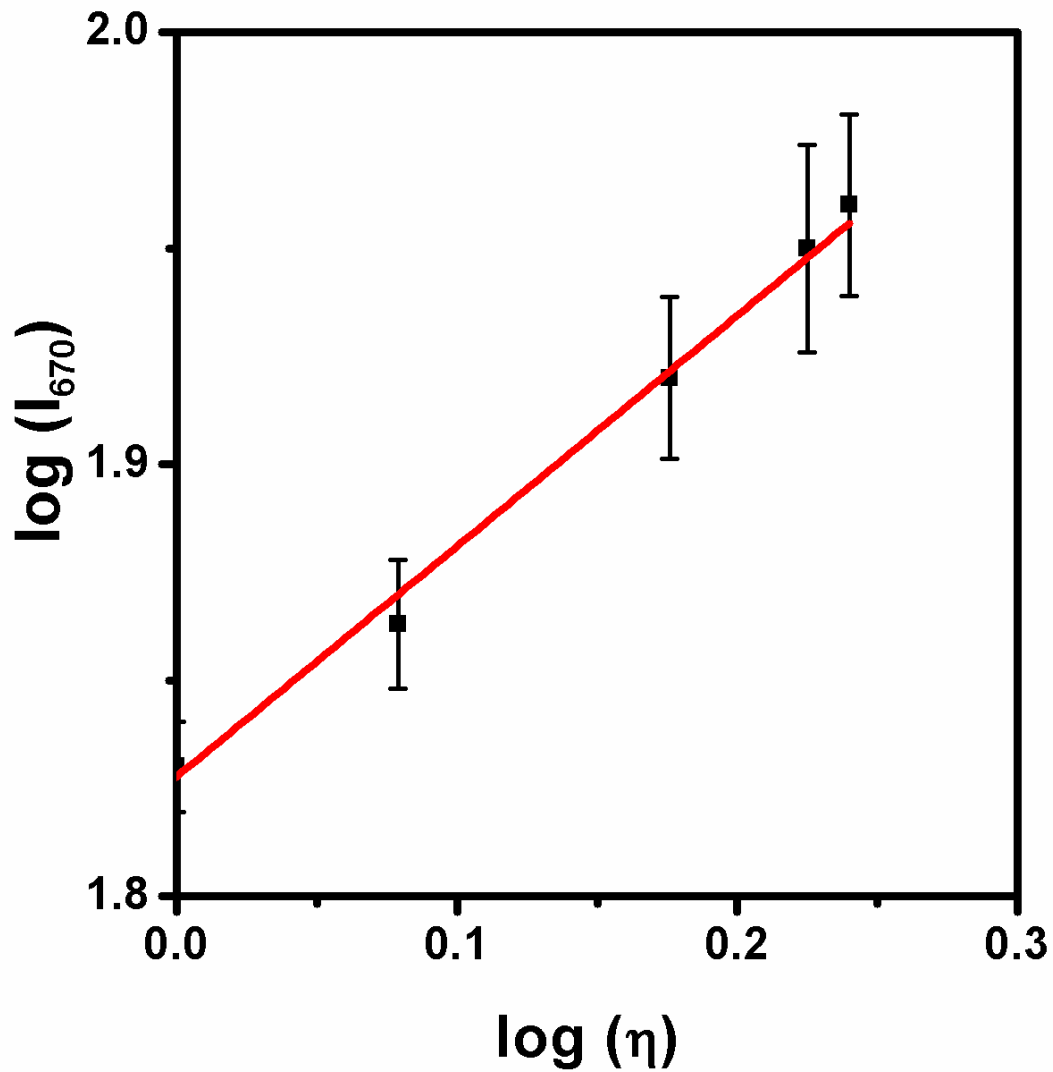
Fig. S9 Detection limit of the sensor DPTMID.

The calibration curve was first obtained from the plot of log (I_{670}) as a function of log
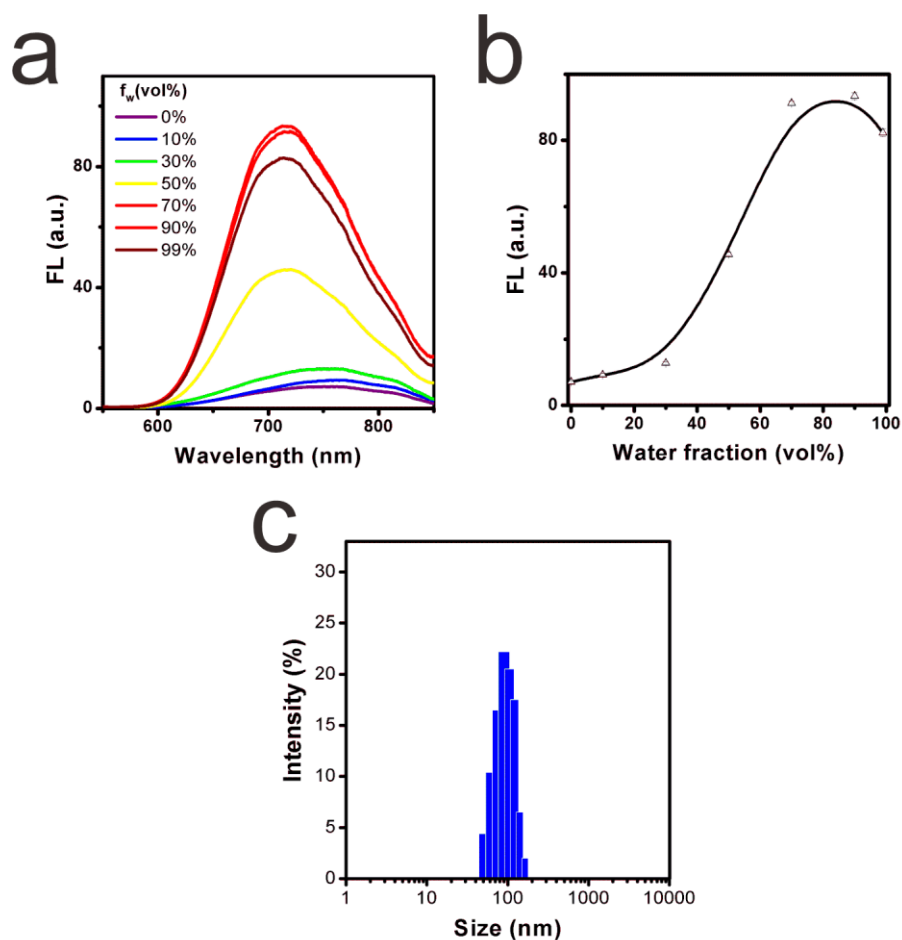
(η). Then the regression curve equation was obtained for the lower viscosity part.

The detection limit $= 3 \times S.D./k$

Where k is the slope of the curve equation, and $S.D.$ represents the standard deviation

for the log (I_{670}) of molecular sensor DPTMID.

log (I_{670}) = 1.821 + 0.532 × log (η) (R^2 = 0.990)

log (LOD) = 3 × 0.0016/0.532 = 0.010

LOD =10^0.010 =1.023 cP
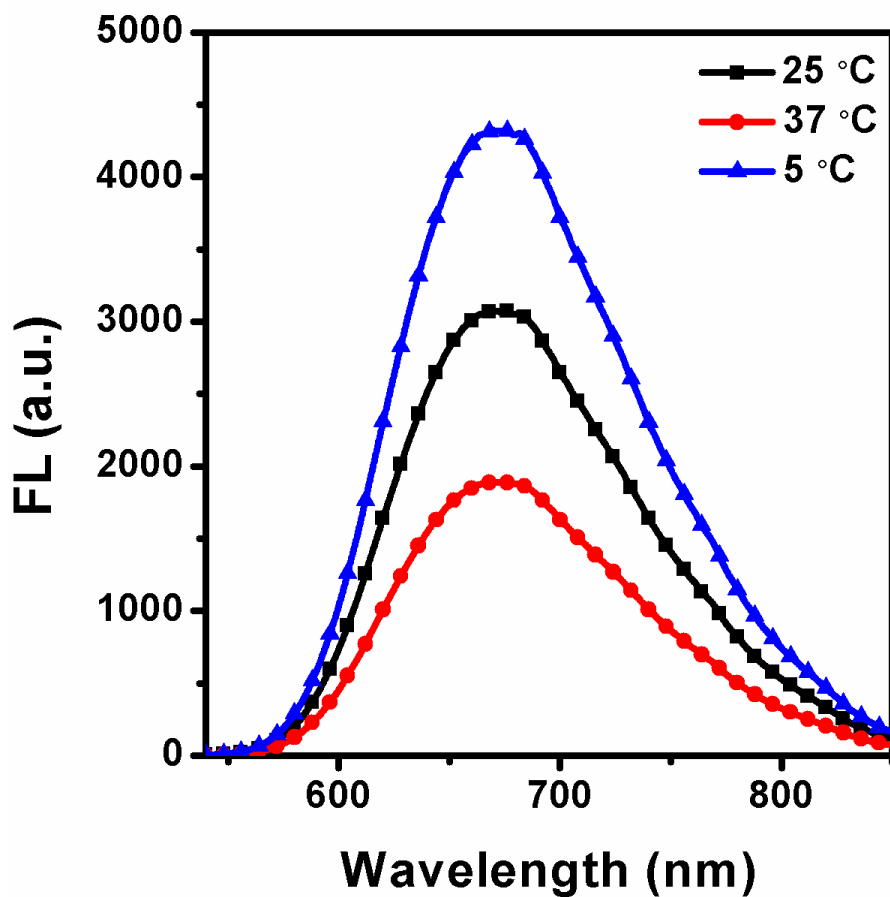
Fig. S10 Fluorescence spectra of the sensor DPTMID (10 μM) in glycerol under different temperature, including the ambient temperature (25 °C), normal body temperature (37 °C), and fresh-maintenance temperature (5 °C).
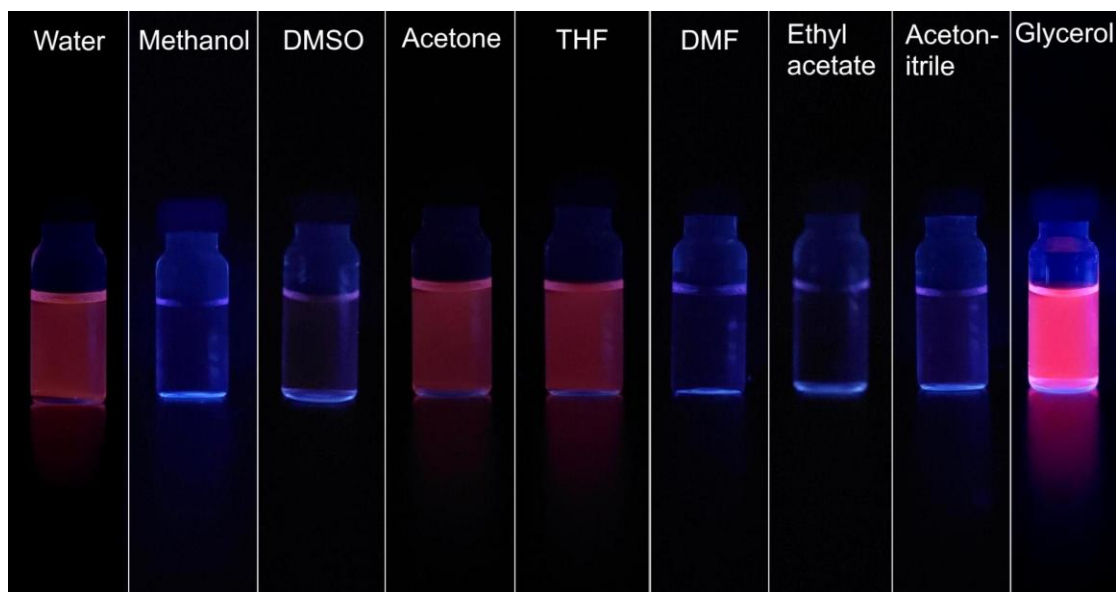
Fig. S11 Fluorescence images of the sensor DPTMID in various solvents.

Fig. S12 Fluorescence emission intensity of the molecular sensor DPTMID (10 μM) at 712 nm under various pH values (containing 1% DMSO) in low viscous water, λ_{ex}=500 nm.

Fig. S13 Photostability analysis of the molecular sensor DPTMID in (a) water (containing 1% DMSO) and other seven kinds of common liquids (containing 1% DMSO). All upon samples were tested under continuous light irradiation with 500 nm UV lamp.
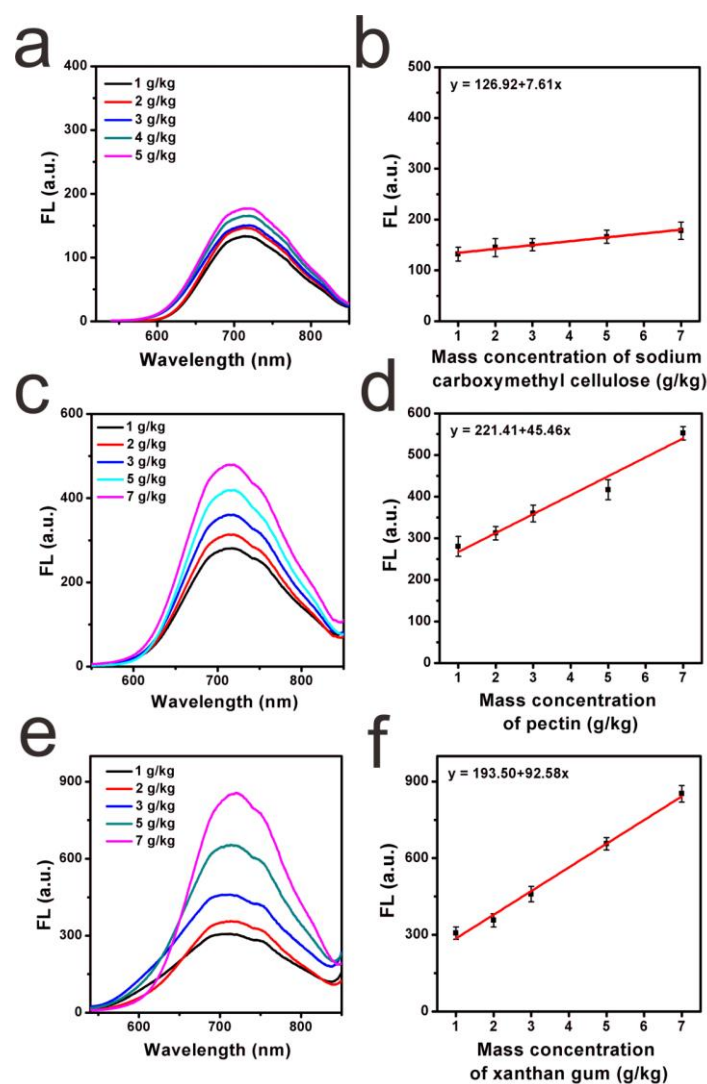
Fig. S14 (a) Fluorescence spectra of the sensor DPTMID in the presence of various mass amounts of sodium carboxymethyl cellulose. (b) Fluorescence intensity of the sensor DPTMID at 714 nm and fitting line with the existence of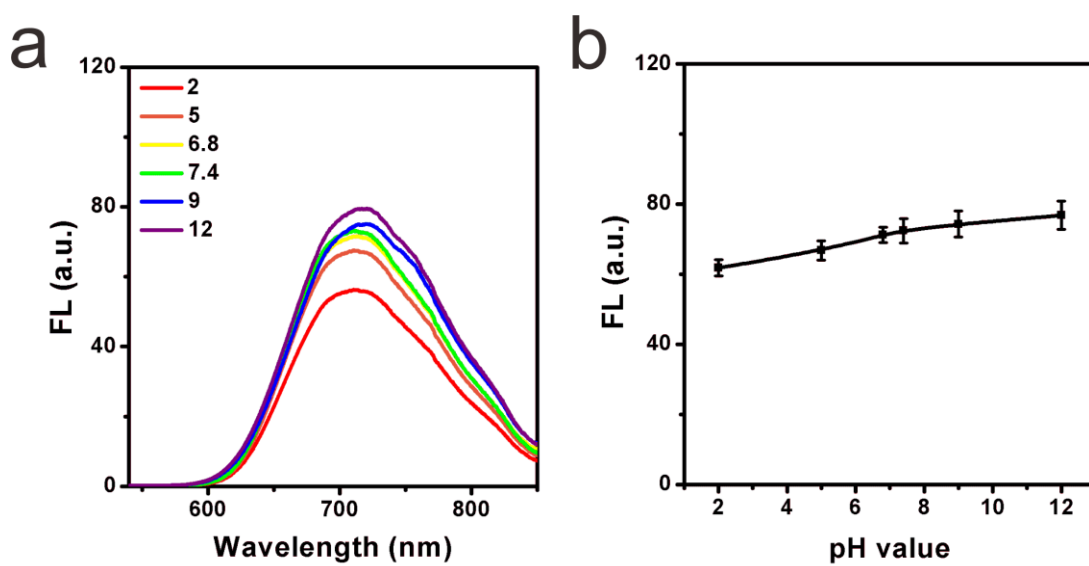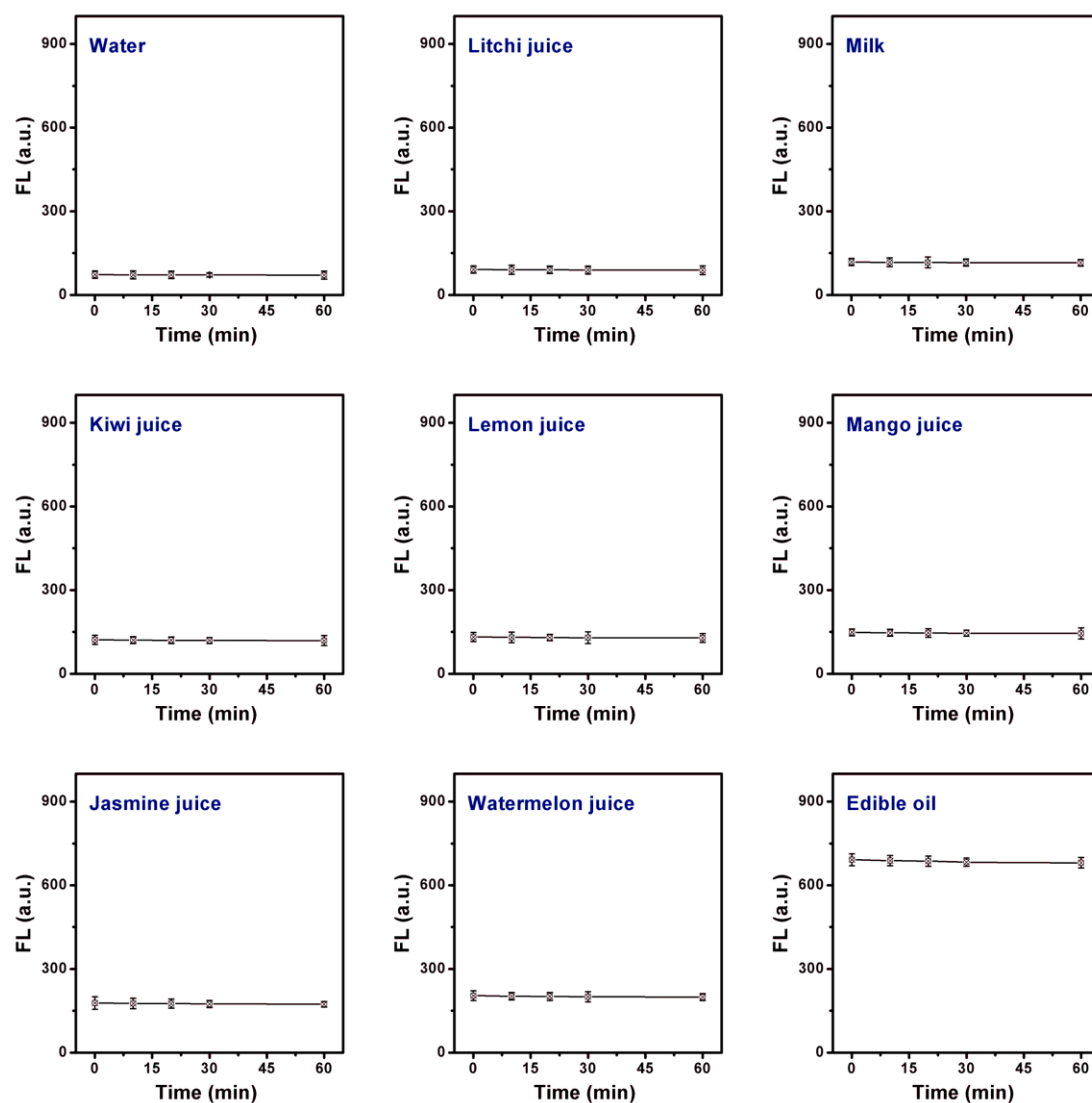 various mass amounts of sodium carboxymethyl cellulose. (c) Fluorescence spectra of the sensor DPTMID in the presence of various mass amounts of pectin. (d) Fluorescence intensity of the sensor DPTMID at 714 nm and fitting line with the existence of various mass amounts of pectin. (e) Fluorescence spectra of the sensor DPTMID in the presence of various mass amounts of xanthan gum. (f) Fluorescence intensity of the sensor DPTMID at 714 nm and fitting line with the existence of various mass amounts of xanthan gum.

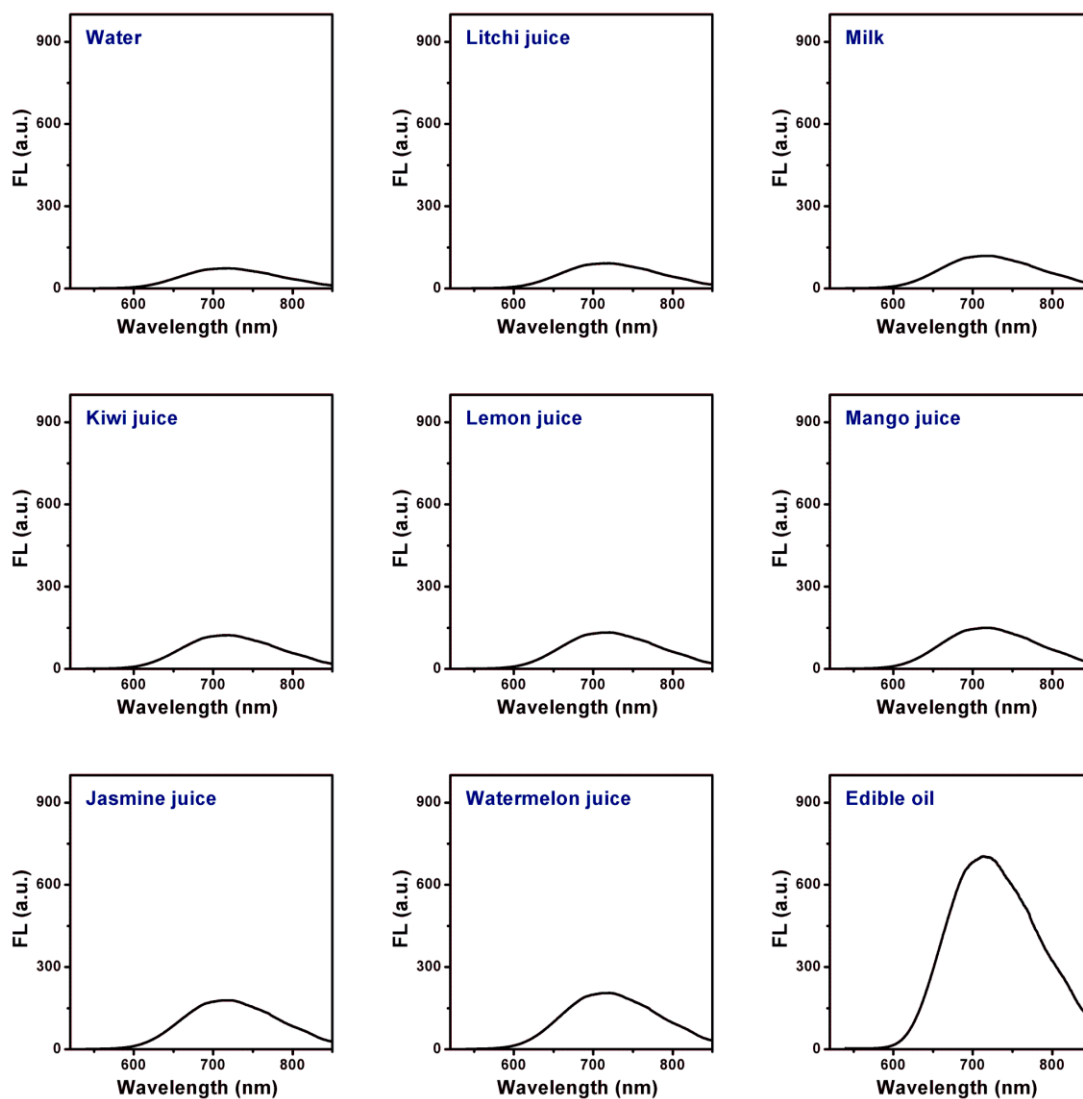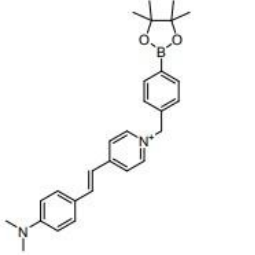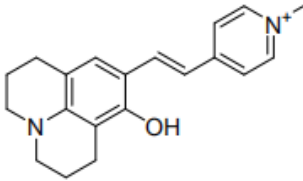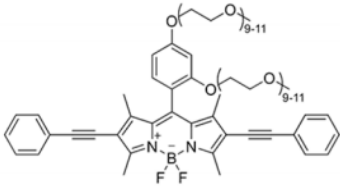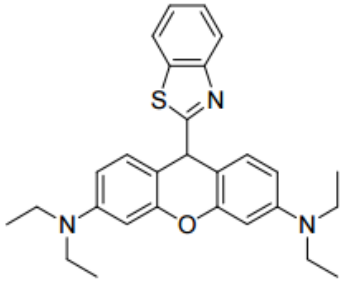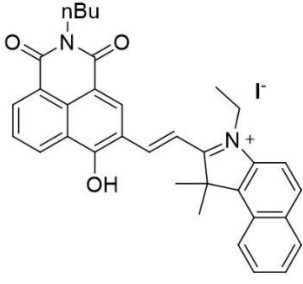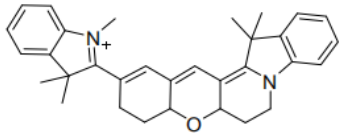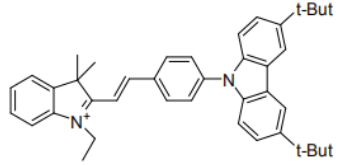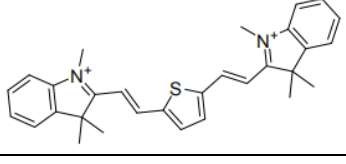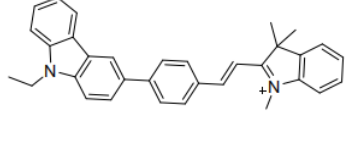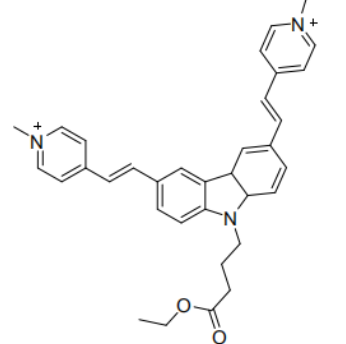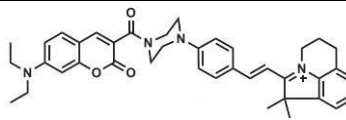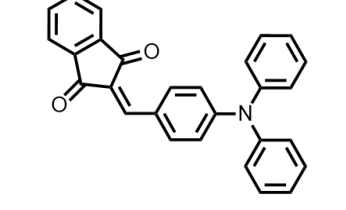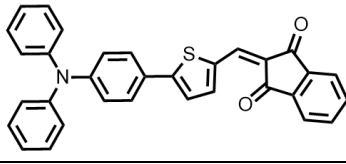**Fig. S15** Fluorescence spectra of the molecular sensor DPTMID (10 μM, containing 1% DMSO) in eight kinds of common liquids, including the water, litchi juice, milk, kiwi juice, lemon juice, mango juice, jasmine juice, watermelon juice and edible oil, λ_{ex}=500 nm.

Table S1. Comparison of the representative fluorescence-based probes for viscosity detection reported in recent years.

Probe	λ_{ab}*	λ_{em}**	Stokes shift***	Application	Reference
	500 nm	607 nm	107 nm	Biological system, living cells.	3
	530 nm	620 nm	90 nm	Biological system, living cells.	4
	560 nm	580 nm	20 nm	Biological system, living cells.	5
	600 nm	635 nm	35 nm	Biological system, living cells, in vivo.	6
	580 nm	635 nm	55 nm	Biological system, living cells.	7
	678 nm	698 nm	20 nm	Biological system, living cells, rat slice.	8

	Absorption*	Emission**	Stokes shift***	Application	Ref.
	545 nm	628 nm	83 nm	Biological system, living cells.	9
	525 nm	595 nm	70 nm	Biological system, living cell.	10
	520 nm	610 nm	90 nm	Biological system, living cell, zebra fish, mice.	11
	470 nm	560 nm	90 nm	Biological system, living cell.	12
	520 nm	580 nm	60 nm	Biological system, living cell.	13
	554 nm	588 nm	34 nm	Liquid food, food spoilage analysis.	This work
	532 nm	670 nm	138 nm	Liquid food, food spoilage analysis.	This work

* Absorption peak. The absorption was measured in the glycerol.

** Emission peak. The fluorescence emission was measured in the glycerol.

*** The stokes shift herein was obtained from the absorption and emission measured in the glycerol.

Table S2. Photo-physical properties of the molecular sensor DPTMID in different solvents.

Solvents	Dielectric constant (ε)	η^* (cP)	Absorption λ_{ab} (nm)	Emission λ_{em} (nm)
Water	78.5	1.0	525.8	710.7
Methanol	32.6	0.6	519.5	/**
DMSO	46.8	2.1	522.8	/
Acetone	20.7	0.4	518.3	701.3
THF	7.4	0.5	511.4	698.3
DMF	36.7	0.8	519.0	/
Ethyl acetate	7.3	0.4	508.2	/
Acetonitrile	37.5	0.4	513.2	/
Glycerol	45.8	956.0	532.2	670.7

* Viscosity of the solvent.

** Non-emissive.

Table S3. Fluorescence intensity of commercial liquids with the molecular rotor DPTMID.

Liquids	Fluorescence intensity
Water	67.14
Litchi juice	90.57
Lemon juice	133.97
Watermelon juice	205.12
Milk	117.50
Jasmine juice	181.55
Mango juice	149.28
Edible oil	707.86
Kiwi juice	124.17

Table S4. Viscosity values of the liquids determined *via* fluorescence technique and viscometer.

Liquids	Viscosity (cP)	Calculated (cP)
Water	1.00	1.02
Litchi juice	1.75	1.81
Lemon juice	3.50	3.42
Watermelon juice	7.50	7.32
Milk	2.81	2.83
Jasmine juice	6.00	5.91
Mango juice	4.22	4.32
Edible oil	68.10	68.21
Kiwi juice	3.04	3.12

References

1   I. E. Steinmark, P.-H. Chung, R. M. Ziolek, B. Cornell, P. Smith, J. A. Levitt, C. Tregidgo, C. Molteni, G. Yahioglu, C. D. Lorenz and K. Suhling, Time-resolved fluorescence anisotropy of a molecular rotor resolves microscopic viscosity parameters in complex environments, *Small*, 2020, **16**, 1907139.

2   F. Liu, Z. Yuan, X. Sui, C. Wang, M. Xu, W. Li and Y. Chen, Viscosity sensitive near-infrared fluorescent probes based on functionalized single-walled carbon nanotubes, *Chem. Commun.*, 2020, **56**, 8301–8304.

3   M. Ren, B. Deng, K. Zhou, X. Kong, J.-Y. Wang and W. Lin, Single fluorescent probe for dual-imaging viscosity and H_2O_2 in mitochondria with different fluorescence signals in living cells, *Anal. Chem.*, 2017, **89**, 552–555.

4   G. Zhang, Y. Sun, X. He, W. Zhang, M. Tian, R. Feng, R. Zhang, X. Li, L. Guo, X. Yu and S. Zhang, Red-emitting mitochondrial probe with ultrahigh signal-to-noise ratio enables high-fidelity fluorescent images in two-photon microscopy, *Anal. Chem.*, 2015, **87**, 12088–12095.

5   L.-L. Li, K. Li, M.-Y. Li, L. Shi, Y.-H. Liu, H. Zhang, S.-L. Pan, N. Wang, Q. Zhou and X.-Q. Yu, BODIPY-based two-photon fluorescent probe for real-time monitoring of lysosomal viscosity with fluorescence lifetime imaging microscopy, *Anal. Chem.*, 2018, **90**, 5873–5878.

6   M. Ren, L. Wang, X. Lv, J. Liu, H. Chen, J. Wang and W. Guo, Development of a benzothiazole-functionalized red-emission pyronin dye and its dihydro derivative for imaging lysosomal viscosity and tracking endogenous peroxynitrite, *J. Mater. Chem. B*, 2019, **7**, 6181–6186.

7   L. Zhu, M. Fu, B. Yin, L. Wang, Y. Chen and Q. Zhu, A red-emitting fluorescent probe for mitochondria-target microviscosity in living cells and blood viscosity detection in hyperglycemia mice, *Dye. Pigment.*, 2020, **172**, 107859.

8   S. J. Park, B. K. Shin, H. W. Lee, J. M. Song, J. T. Je and H. M. Kim, Asymmetric cyanine as a far-red fluorescence probe for mitochondrial viscosity, *Dye. Pigment.*, 2020, **174**, 108080.

9   K. Zhou, M. Ren, B. Deng and W. Lin, Development of a viscosity sensitive fluorescent probe for real-time monitoring of mitochondria viscosity, *New J. Chem.*, 2017, **41**, 11507–11511.

10 Y. Baek, S. J. Park, X. Zhou, G. Kim, H. M. Kim and J. Yoon, A viscosity sensitive fluorescent dye for real-time monitoring of mitochondria transport in neurons, *Biosens. Bioelectron.*, 2016, **86**, 885–891.

11 J. Yin, M. Peng and W. Lin, Visualization of mitochondrial viscosity in inflammation, fatty liver, and cancer living mice by a robust fluorescent probe *Anal. Chem.*, 2019, **91**, 8415–8421.

12 Z. Zou, Q. Yan, S. Ai, P. Qi, H. Yang, Y. Zhang, Z. Qing, L. Zhang, F. Feng and R. Yang, Real-time visualizing mitophagy-specific viscosity dynamic by mitochondria-anchored molecular rotor, *Anal. Chem.*, 2019, **91**, 8574–8581.

13 L. He, Y. Yang and W. Lin, Rational design of a rigid fluorophore–molecular rotor-based probe for high signal-to-background ratio detection of sulfur dioxide in viscous system, *Anal. Chem.*, 2019, **91**, 15220–15228.